BRUECKNER-BETHE CALCULATIONS OF NUCLEAR MATTER

by

B. D. Day

Prepared for

IAEA Conference on

"Recent Progress in Many-Body Theories"

Trieste, Italy

October 2-7, 1978

UNC-AUA-USDOE

ARGONNE NATIONAL LABORATORY, ARGONNE, ILLINOIS

Operated under Contract W-31-109-Eng-38 for the

U. S. DEPARTMENT OF ENERGY

BRUECKNER-BETHE CALCULATIONS OF NUCLEAR MATTER[†]

B. D. DAY

Argonne National Laboratory, Argonne, IL. 60439 USA[*]

Abstract: The ideas of the Brueckner-Bethe hole-line expansion are briefly outlined. Four practical tests of its validity are formulated. These tests are applied to recent numerical results for the central potential v_2 and the semirealistic potential v_6(Reid), which contains a tensor force but no spin-orbit force. The results are consistent with the validity of the hole-line expansion. The Brueckner-Bethe results are also consistent, within uncertainties of order 3 MeV, with variational results.

[†]Invited talk at the Conference on "Recent Progress in Many-Body Theories," October, 1978, at the International Center for Theoretical Physics, Trieste, Italy.

[*]Work performed under the auspices of the U. S. Dept. of Energy.

I. Introduction

In nuclear matter theory we start with a model of the nucleus. We consider it to be composed of point nucleons interacting through a two-body potential that is fitted to scattering data and to the properties of the deuteron. Then we ask whether this model can account for the saturation properties of nuclear matter. To answer this question we must be able to solve the equations of the model. This means, given a two-body potential, that we must be able to calculate the energy per particle as a function of density and find the minimum of this curve - the saturation point. At the present time we are still in the process of developing an adequate method of calculation. The two methods that have received most attention are the Brueckner-Bethe method[1-6] and the variational method[6-10]. In this paper I give my view of the present state of the Brueckner-Bethe method. First the method is briefly outlined. Then numerical results are presented that have a bearing on whether the method is valid, on what numerical accuracy is attainable, and on the comparison of the method with the variational method.

II. Outline of the Brueckner-Bethe method

The presently most powerful and flexible formulation of the Brueckner-Bethe method is that of the coupled-cluster equations, alternatively called the exp(S) equations, of Coester[11] and Kümmel[12]. The calculations to be described here correspond to a particular approximation scheme for the solution to these equations. This scheme is called the hole-line expansion and is conveniently described in terms of Goldstone diagrams[1,13]. This is the procedure followed here. However, for the purpose of formulating other approximation schemes, and for theoretical

investigation of convergence, it is probably best to use the coupled-cluster equations rather than the Goldstone diagrams.

The Hamiltonian H is given by the sum of the kinetic energies of the nucleons and the two-body interactions among them:

$$H = \sum_{i=1}^{A} T_i + \sum_{i<j}^{A} v_{ij} \quad . \tag{1}$$

We write this in the form

$$H = H_0 + H_1 \tag{2}$$

where

$$H_0 = \sum_{i=1}^{A} (T_i + U_i) \tag{3}$$

$$H_1 = \sum_{i<j}^{A} v_{ij} - \sum_{i=1}^{A} U_i \tag{4}$$

Here, U is a single-particle potential that is at our disposal. It should be chosen so that whatever expansion we use for the energy converges well. We assume translational invariance so that U is diagonal in momentum space. Then the single-particle energy of a plane-wave state of momentum $\vec{k}$ is given by

$$E(k) = \hbar^2 k^2/2M + U(k) \quad . \tag{5}$$

The Fermi-gas state Φ satisfies

$$H_0 \Phi = \mathcal{E}_0 \Phi \tag{6}$$

where

$$\mathcal{E}_0 = \sum_{k<k_F} E(k) \quad . \tag{7}$$

The exact ground-state wavefunction Ψ satisfies

$$H\Psi = \mathcal{E}\Psi \tag{8}$$

and the exact ground-state energy $\mathcal{E}$ is given formally by the sum of all linked Goldstone diagrams[13].

The contribution of any diagram contains energy denominators, and the energy denominators depend on the single-particle spectrum E(k), which is plotted in fig. 1. For k less than the Fermi momentum k_F, U(k) is defined as in Hartree-Fock theory, and the single-particle energy is negative. For $k>k_F$ the conventional choice is U(k) = 0. This gives the solid curve in fig. 1, which has a gap of order 50 MeV at the Fermi surface. Spectra that are more nearly continuous at the Fermi surface, such as the dashed curve, have also been used[14,15]. The choice of U will be discussed more fully later.

Since we want to be able to treat potentials with a strong short-range repulsion, we must eliminate the potential v in favor of the two-body reaction matrix G, which satisfies the equation

$$G = v - v(Q/e)G \quad . \tag{9}$$

Here, e is defined by

$$e|pq\rangle = (E(p) + E(q)-\omega)|pq\rangle \ , \tag{10}$$

where $|pq\rangle$ is a product of two single-particle plane waves, and the starting energy ω depends on the details of the diagram in which the interaction occurs[1].

The relative wavefunction for two noninteracting particles is a plane wave ϕ, and the correlated wavefunction is then defined by

$$\psi = \phi - (Q/e)G\phi \quad . \tag{11}$$

Eqs. (9) and (11) give

$$v\,\psi = G\,\phi \quad . \tag{12}$$

From this equation, we see that if v becomes very large at small r, then ψ becomes small so that G remains well behaved.

The behavior of ψ is crucial for the Brueckner-Bethe method. Fig. 2 shows this behavior for two particles in the $^3S_1$-$^3D_1$ channel interacting through the Reid[16] potential. The uncorrelated wavefunction ϕ has been chosen to have only an S-wave component given by

$$\phi = j_0(kr) \quad , \tag{13}$$

where k is the relative momentum. Since the tensor force couples the $^3S_1$ state to the $^3D_1$ state, ψ has both S- and D- wave components, denoted by ψ_S and ψ_D, respectively.

At small r, ψ_S becomes small because of the strong short-range repulsion. So in this region we have strong correlations in the sense that ϕ-ψ is comparable to ϕ. But for $r \gtrsim 0.5$ fm, the correlations are weak in the sense that $|\phi-\psi| \ll \phi$. Since the D-wave part of ϕ is zero, the D-state correlations are entirely given by ψ_D. Again, these correlations are weak in the sense that $|\psi_D| \ll \phi$. The essential point is that the strong correlations have a very short range (comparable to the range of the short-range repulsion), and the longer-range correlations are very weak.

A useful measure of the strength of the correlations is the correlation volume defined by

$$\text{corr. vol.} = \int |\phi-\psi|^2 d\tau \quad . \tag{14}$$

Dividing this by the volume per particle, which is equivalent to multiplying by the density ρ, defines the dimensionless parameter κ_2:

$$\frac{\text{corr. vol.}}{\text{vol. per particle}} = \rho \int |\phi-\psi|^2 d\tau = \kappa_2 \qquad (15)$$

For the Reid potential, κ_2 ranges from 0.15 to 0.25 for $\rho_o \leq \rho \leq 2\rho_o$, where ρ_o is the empirical saturation density of nuclear matter. These values are calculated using the conventional single-particle spectrum with a large gap at the Fermi surface. With a more nearly continuous spectrum one may find values of κ_2 that are 20% larger.

In any case, the ratio κ_2 of the correlation volume to the volume per particle is much less than 1, and this fact has the following interpretation. If two particles are correlated, the probability that a third particle will be correlated with the first two is of the order of this ratio and is therefore small compared to 1. This suggests grouping the energy diagrams according to the number of interacting particles — first two-body correlations, then three-body correlations, etc. The number of interacting particles is equivalent to the number of hole lines, so this leads to the hole-line expansion:

$$\mathcal{E}/A = \overline{T} + D_2 + D_3 + \ldots \qquad (16)$$

The leading term $\overline{T}$ is the kinetic energy of the Fermi-gas state, and D_n is the contribution from diagrams with n hole lines.

Each additional hole line involves an integration over momenta in the Fermi sea and gives a factor of the density. On dimensional grounds this must be multiplied by some correlation volume to give a factor of order κ_2. One can give more detailed arguments like this[1], but the real test of the hole-line expansion is to try it out and see if it works. So let us look at this expansion in more detail.

For the kinetic energy of the Fermi-gas state one finds

$$\overline{T} = 25 \text{ to } 40 \text{ MeV for } \rho_o \leq \rho \leq 2\rho_o \,. \qquad (17)$$

The two-hole-line term D_2 is represented by the diagram of fig. 3. It represents the interaction between each pair of particles in the Fermi sea and is given by

$$D_2 = \sum_{m<n<k_F} \langle mn|G|mn\rangle \sim -40 \text{ MeV} \quad . \tag{18}$$

The value of D_2 depends on both the two-body potential and the density, and -40 MeV is a typical value.

The three-hole-line diagrams are shown in figs. 4 and 5. The wiggly lines represent the two-body reaction matrix G and the dashed line with a cross represents the single-particle potential U. Upward directed lines represent occupied states above the Fermi sea, and downgoing lines represent empty states (holes) in the Fermi sea. The rules for associating an energy contribution to a diagram are discussed in ref. 1. As an example, the contribution from fig. 4(a) is

$$- \sum_{\substack{\ell,m,n<k_F \\ a,b\ >k_F}} \langle \ell m|G|ab\rangle \ (E_a+E_b-E_\ell-E_m)^{-2} \ \langle mn|G|mn\rangle \ \langle ab|G|\ell m\rangle . \tag{19}$$

The contribution of fig. 4(a) is large, typically +10 to +15 MeV. Fig. 4(b) is identical with fig. 4(a) except for the middle interaction. These two diagrams can be made to exactly cancel by choosing U(m) for $m<k_F$ to be

$$U(m) = \sum_{n<k_F} \langle mn|G|mn\rangle \ , \ m<k_F \quad . \tag{20}$$

Eq. (20) is our choice of U(m) for $m<k_F$.

Fig. 4(c) is called the hole-hole diagram D_2^{hh}. It has four hole lines, but momentum conservation in the middle interaction means that only three of these momenta are independent. So we have only three independent integrations over the Fermi sea, and this diagram is therefore considered

to be a three-hole-line diagram. It contributes less than 1 MeV and is therefore not very important.

In fig. 4(d) a particle above the Fermi sea interacts with the single-particle potential. With the conventional spectrum, we have $U(b) = 0$ for $b > k_F$ so that fig. 4(d) is zero. But if a non-zero U is used above the Fermi sea, then fig. 4(d) should be evaluated as a three-hole-line diagram, just as fig. 4(b) was used to cancel a three-hole-line diagram.

The last term in D_3 is the three-body cluster term D_3^c. It contains an infinite number of diagrams, some of which are shown in fig. 5. There are 2 diagrams of third order in G, 4 of the fourth order, etc. A typical example is shown in fig. 5(g). In the first two interactions at the bottom, three particles are excited above the Fermi sea. Then many interactions are drawn between the upgoing particle lines, and finally at the top the three excited particles fall back into the sea. Although there are many interactions in this diagram, there are only three hole lines.

For two-body potentials with a strong short-range repulsion, it is known that the series of three-body cluster diagrams does not converge[1,17,18] but must be summed by solving the three-body Bethe-Faddeev equations. This gives one reason for the conventional choice $U(k) = 0$ for $k>k_F$. If we wanted to define U so that fig. 4(d) cancels fig. 5(a), this could be conveniently done. But fig. 5(a) is no more important than any other three-body cluster diagram, all of which must be grouped together in a single term D_3^c. And there is no natural and convenient way to make fig. 4(d) cancel the more complicated three-body cluster diagrams. Therefore, we do not attempt such a cancellation but simply put $U(k) = 0$ for $k>k_F$ and then evaluate D_3^c explicitly.

So with the conventional single-particle spectrum, figs. 4(a) and 4(b) cancel, fig. 4(d) is zero, and we are left with the very small hole-hole term D_3^{hh} of fig. 4(c) and the three-body cluster term D_3^c of fig. 5.

We come next to four-hole-line diagrams. These have been enumerated[19,20], and many have been calculated[19]. I will discuss them further in connection with the numerical results.

The question of how to choose U allows us to formulate a test of the hole-line expansion. The idea is due to Mahaux[21]. Suppose we change U by adding a constant Δ to the single-particle potential of every state above the Fermi sea. Then the calculated energy will change. For example, we have

$$\frac{\partial D_2}{\partial \Delta} = \kappa_2 \sim 0.2 \quad . \tag{21}$$

However, the exact energy cannot depend on our choice of U and is therefore independent of Δ. This suggests that as we include more terms in the hole-line expansion, the sensitivity of the calculated energy to Δ should become smaller and smaller. In particular, we require that

$$\left| \frac{\partial (D_2+D_3)}{\partial \Delta} \right| << \left| \frac{\partial D_2}{\partial \Delta} \right| = \kappa_2 \quad . \tag{22}$$

If we calculate D_2 and D_3, we can check whether the condition (22) is satisfied[6]. Thus we have a practical test of the hole-line expansion.

Another important test is to look for the possible buildup of long-range correlations. One usually expects these to come from the ring diagrams, as in the electron gas[22] and in low-density Bose systems[23]. In nuclear matter, however, the situation is more complicated. This can be seen by looking again at the three-body cluster diagrams in fig. 5.

Only one of these, namely fig. 5(b), is a ring diagram. Yet we know that all these diagrams have to be grouped together in a single term. By removing the first and last interactions from fig. 5(b) we obtain the ring vertex of fig. 6(c). It must be kept together with fig. 6(b) and with all the diagram structures obtained by removing the first and last interactions from more complicated three-body cluster diagrams.

We define M to be the sum of all these diagram structures, as shown in fig. 6. Then instead of iterating the ring vertex 6(c), which would generate ring diagrams, we iterate M and generate a series of generalized ring diagrams. The first term in the generalized ring series is fig. 7(a), which is just the three-body cluster term D_3^c. The term of second order in M (shown in fig. 7(b)) is the four-hole-line diagram of class B1 in the notation of ref. 19, and each succeeding term is represented by diagrams with one additional hole line. Thus, according to the ideas of the hole-line expansion, this series should converge rapidly. But if long-range correlations are important, it may converge badly. Then the entire series would have to be summed at once into a single term. The calculation has been done for light nuclei by Zabolitzky[24], who finds that the generalized ring series converges rather slowly. It is important to carry out the same test for nuclear matter.

This completes our outline of the ideas of the hole-line expansion. We have four practical tests to apply to this method:

1) Do the first three terms of the expansion converge well?
2) Is condition (22) satisfied?
3) Does the generalized ring series converge well?
4) For simple central potentials, reliable Monte-Carlo variational calculations exist[25], and we can check whether the results of the hole-line expansion are consistent with these.

III. Numerical results

The numerical results to be presented require solving the three-body Bethe-Faddeev equations[18]. This has been done using a method developed previously[26], and further details will be given elsewhere[27]. Here I make only two remarks about the calculational method.

First, the three-body equations are not solved exactly. Several approximations are made, the main one being the use of an angle-average Pauli operator. I expect a numerical uncertainty of order 2 MeV at $k_F = 1.8$ fm^{-1} (corresponding to $\rho = 2\rho_o$) and of order 0.5 MeV at $k_F = 1.4$ fm^{-1} ($\rho \approx \rho_o$).

Second, the complexity of the nuclear force presents no problem in the three-body calculations. Tensor forces, spin-orbit forces, quadratic spin-orbit forces, etc., can all be properly treated.

All the numerical results given below have been obtained using the conventional single-particle spectrum with $U(k) = 0$ for $k>k_F$.

Let us first consider the potential v_2[28]. It is a central potential with no spin or isospin dependence and has a Yukawa-shaped repulsive core followed by a weak attractive force.

In order to apply the tests listed at the end of Sec. II, we look at the results for $k_F = 1.8$ fm^{-1}. Since this corresponds to a density of twice the empirical saturation density of nuclear matter, and since we find $\kappa_2 = 0.27$, which is rather large, this case should provide a stringent test of the hole-line expansion. The results are shown in table 1 (the calculation of D_4 and of the numerical uncertainty in the total are described later). The three-hole-line contribution D_3 is the sum of $D_3^{c} = -9.6$ MeV and $D_3^{hh} = -0.6$ MeV.

Table 1 shows good convergence of the hole-line expansion. Note also that $D_3 = -10.2$ MeV is comparable to $\kappa_2 D_2 = -8.2$ MeV. Thus the rate of convergence is roughly governed by the size of κ_2, which is in accord with the ideas of the hole-line expansion.

Condition (22) is tested in table 2. We see that including the three-hole-line contribution greatly reduces the sensitivity of the calculated energy to a shift Δ of the intermediate-state spectrum. This is consistent with the validity of the hole-line expansion.

The individual contributions to the three-body cluster term D_3^c are shown in table 3. The columns labeled "bubble" and "ring" refer to the third-order diagrams of figs. 5(a) and 5(b), respectively. The column labeled "higher" gives the sum of all higher-order three-body cluster diagrams. It is clear that omitting these higher-order diagrams, which can only be evaluated by solving the three-body equations, would give completely wrong results.

To search for long-range correlations, we look at the convergence of the generalized ring series, which is shown in table 4. The contribution of first order in M is D_3^c, and the second-order term is the four-hole-line diagram of class B1 shown in fig. 7(b), which we denote by D_4 (B1). Each term in the generalized ring series has one more hole line than its predecessor. The convergence is seen to be rapid: adding a hole line greatly reduces the contribution of the diagram. Also, the sum to infinite order of the generalized ring series is found to be -11.6 MeV, which is just equal to the partial sum of the first 4 terms. Thus there is no indication here that we need to depart from the grouping of diagrams strictly according to the number of hole lines.

The four-hole-line diagram D_4(B1) is just one of a number of four-hole-line diagrams. Approximate formulas for most of these have been obtained in an earlier paper[19]. Using the results in that paper, I have estimated all of the four-hole-line diagrams and their numerical errors. Then I

have estimated the total numerical error by summing the squares of the individual errors and taking the square root. This gives the value for D_4 in table 1. The numerical uncertainty quoted for the total in table 1 comes from both D_3 and D_4.

The most questionable part of this procedure involves the four-body cluster term, which is the only four-hole-line term that requires solving a four-body equation. For this term I have assumed a value of zero with an uncertainty of $\pm \kappa_2^2 D_2$. This is consistent with available numerical estimates[19,29], but the accuracy of these estimates is not well-established. I feel that the total numerical uncertainty of ± 2.5 MeV quoted in table 1 is reasonable, but more work is needed to pin it down better.

The results for v_2 are plotted as a function of density in fig. 8. The curve labeled BB(2) includes only $\overline{T} + D_2$. Adding D_3 gives the curve BB(3), and adding D_4 to this gives the curve BB(4). The dashed lines give my estimate of the numerical uncertainty in the BB(4) result. The solid circles with error bars give the variational upper bounds obtained by Ceperley, Chester, and Kalos[25] using the Monte-Carlo method. We see that the Brueckner-Bethe results lie somewhat below the variational upper bounds, which is consistent with the validity of the hole-line expansion.

Thus we see that for v_2 the four tests mentioned at the end of Sec. II give no indication of trouble with the hole-line expansion. The first three terms converge well, condition (22) is well satisfied, the generalized ring series converges well, and the results are consistent with variational upper bounds.

These results are sufficiently encouraging that it makes sense to apply the method to a more realistic potential. I have selected the potential v_6(Reid) for this purpose. It has been used in variational calculations by the Illinois group[30] and is defined as follows. In all singlet-even

states the radial shape is that of the $^1S_0$ Reid[16] soft-core potential. In all singlet-odd states, the Reid $^1P_1$ potential is used. In triplet-even states the form $V_C(r)+V_T(r)S_{12}$ is used, where S_{12} is the tensor operator. The radial shapes of V_C and V_T are those of the Reid $^3S_1$-$^3D_1$ potential. In triplet-odd states the definition is similar, with $V_C(r)$ and $V_T(r)$ taken from the Reid $^3P_2$-$^3F_2$ potential. The spin-orbit force has been omitted because it gives trouble for the variational calculations at their present state of development. The spin-orbit force would not be troublesome in the Brueckner-Bethe method, however.

Let us first look at the results for $k_F = 1.8$ fm^{-1}, corresponding to a density more than twice the empirical saturation density. The calculated value of κ_2 is 0.25, and the various contributions to the energy are shown in table 5. The convergence of the first three terms of the hole-line expansion is seen to be good. The three-hole-line term D_3 is the sum of $D_3^c = -13.5$ MeV and $D_3^{hh} = -0.9$ MeV. The value of D_3 is comparable to $\kappa_2 D_2 = -11.2$ MeV, in accord with the ideas of the hole-line expansion. Table 6 shows that condition (22) is well satisfied, which also supports the validity of the hole-line expansion.

The individual contributions to the three-body cluster term D_3^c are shown in table 7. Again it is essential to include the higher-order diagrams, which requires solving the three-body Bethe-Faddeev equations.

The convergence of the generalized ring series is shown in table 8. The convergence is rapid, and the sum to infinite order is found to be -15.9 MeV, which is equal to the partial sum of the first four terms. This is somewhat surprising because the two-body potential has a strong tensor force that might be expected to build up appreciable long-range correlations. However, this possibility does not seem to materialize.

The results in table 8 give no indication that we should modify the hole-line expansion.

The results for v_6(Reid) are plotted as a function of density in fig. 9. The curves labeled BB(2), BB(3), BB(4), and also the dashed curves, have the same meaning as in fig. 8. The curve labeled PW is the variational calculation of Pandharipande and Wiringa[30]. The crosses show the minima of the curves as determined by eye. The difference between the Brueckner-Bethe result and the variational result of the Illinois group is about 3 MeV and can certainly be accounted for by the combined uncertainties in the two calculations.

Let us now summarize the main results for the two-body potential v_6(Reid). The first three terms of the hole-line expansion show good convergence. The sensitivity of the calculated energy to a shift in the intermediate-state spectrum is satisfactorily reduced when the three-hole-line term is added to the two-hole-line term. The generalized ring series converges rapidly, suggesting that long-range correlations do not spoil the hole-line expansion. Finally, although no Monte-Carlo variational upper bounds are available for v_6(Reid), the Brueckner-Bethe results are consistent with the variational calculation of the Illinois group.

IV. Summary and discussion

Using the ideas developed at the end of Sec. II, we have made several tests of the Brueckner-Bethe hole-line expansion. This has been done for two different two-body potentials: the simple central potential v_2[28] and the semirealistic potential v_6(Reid)[30], which has a tensor force. No indication of trouble with the hole-line expansion is found. This suggests, but does not prove, that the hole-line expansion is a valid method.

A reasonable, but not firmly established, estimate of the error in the present calculations is 3 MeV at twice the empirical saturation density (k_F = 1.8 fm^{-1}), and the error decreases at lower densities. We are thus getting close to the point where the method can tell us what we really want to know, i.e., which two-body potential, if any, can account for the saturation properties of nuclear matter.

However, there is much room for improvement. On the technical side, a calculation of the four-body cluster term would be extremely useful. This may be very difficult because it requires solving a four-body equation. But even a reliable estimate or bound for this term would be valuable. Improving the calculation of the other four-hole-line terms and of the three-hole-line terms would also be valuable technical improvements.

On the theoretical side, we need to understand the energy expansion better. For example, with the v_6(Reid) two-body potential, at k_F = 1.8 fm^{-1}, there are several four-hole-line diagrams that are 2-3 MeV in magnitude. But because of cancellations among these terms, the total four-hole-line contribution is only about 2 MeV. How does this come about, and will it also happen for higher-order terms? I don't have a good answer to this question, but one is clearly needed. Probably the coupled-cluster equations[11,12] will be useful in attacking this problem.

Let us close by briefly comparing the Brueckner-Bethe and variational methods. For simple central potentials, the variational approach is more efficient[6]. With powerful partial-summation methods such as the Fermi hypernetted-chain method[31-33], one can calculate reliably at higher densities than with the Brueckner-Bethe method. However, as the two-body potential gets more complicated, it becomes harder and harder to carry out these partial summations in the variational method. At the present time, for example, the spin-orbit force is very troublesome in variational calculations[30].

In the Brueckner-Bethe method, on the other hand, the most general two-body potential can be treated without difficulty.

Thus, at the present time, each of the two methods has its strengths and weaknesses. The method that eventually emerges may be one of these, or it may be something like the recent approach of the Clark-Ristig group[34], which combines a variational calculation with perturbation theory. For the present it is highly desirable that a variety of methods be developed and compared with each other.

Table Captions

1. Calculated energy contributions in MeV for the two-body potential v_2 at $k_F = 1.8$ fm^{-1}.
2. Sensitivity of calculated energy to a shift in the spectrum for v_2 at $k_F = 1.8$ fm^{-1}.
3. Various contributions to D_3^c in MeV for v_2 ($k_F = 1.8$ fm^{-1}), as discussed in the text.
4. Contributions in MeV of various terms in the generalized ring series for v_2 ($k_F = 1.8$ fm^{-1}), as discussed in the text.
5. Calculated energy contributions in MeV for the two-body potential v_6(Reid) at $k_F = 1.8$ fm^{-1}.
6. Sensitivity of calculated energy to a shift in the spectrum for v_6(Reid) at $k_F = 1.8$ fm^{-1}.
7. Various contributions in MeV to D_3^c for v_6(Reid) at $k_F = 1.8$ fm^{-1}.
8. Convergence of generalized ring series for v_6(Reid) at $k_F = 1.8$ fm^{-1}.

Table 1

$\overline{T}$	D_2	D_3	D_4	total
40.3	-30.5	-10.2	+1.4	+1.0 ± 2.5

Table 2

$\partial D_2/\partial\Delta$	$\partial(D_2+D_3)/\partial\Delta$
0.27	0.02 ± 0.03

Table 3

bubble	ring	higher	total = D_3^c
+6.9	+17.2	-33.7	-9.6

Table 4

order in M	1	2	3	4
energy	-9.6	-2.1	+0.4	-0.3
remarks	D_3^c	D_4(B1)	5 hole lines	6 hole lines

Table 5

$\overline{T}$	D_2	D_3	D_4	total
40.3	-45.7	-14.4	+2.0	-17.8 ± 3.3

Table 6

$\partial D_2/\partial\Delta$	$\partial(D_2+D_3)/\partial\Delta$
0.25	0.01 ± 0.03

Table 7

bubble	ring	higher	total = D_3^c
+22.2	-18.6	-17.1	-13.5

Table 8

order in M	1	2	3	4
energy	-13.5	-2.0	-0.3	-0.07
remarks	D_3^c	D_4(B1)	5 hole lines	6 hole lines

References

1) B. D. Day, Rev. Mod. Phys. 39(1967) 719

2) H. A. Bethe, Ann. Rev. Nucl. Sci. 21(1971) 93

3) D. W. Sprung, Adv. Nucl. Phys. 5(1972) 225

4) H. S. Köhler, Phys. Rept. 18C(1975) 217

5) J.-P. Jeukenne, A. Lejeune and C. Mahaux, Phys. Rept. 25C(1976) 84

6) B. D. Day, Rev. Mod. Phys. 50(1978) 495

7) J. W. Clark, Prog. in Particle and Nuclear Physics, to be published

8) R. B. Wiringa and V. R. Pandharipande, Nucl. Phys. A299(1978) 1

9) O. Benhar, C. Ciofi degli Atti, S. Fantoni and S. Rosati, Phys. Lett. 70B(1977) 1

10) J. C. Owen, Ann. Phys. (N.Y.) to be published

11) F. Coester, in Lectures in Theoretical Physics: Quantum Fluids and Nuclear Matter, edited by K. T. Mahanthappa and W. E. Brittin (Gordon and Breach, New York) (1969) Vol. XI B

12) H. Kümmel, K. H. Lührmann and J. G. Zabolitzky, Phys. Rept. 36C(1978) 1

13) J. Goldstone, Proc. Roy. Soc. A239(1957) 267

14) H. S. Köhler, Nucl. Phys. A204(1973) 65

15) A. Lejeune and C. Mahaux, Nucl. Phys. A295(1978) 189

16) R. V. Reid, Ann. Phys. (N.Y.) 50(1968) 411

17) H. A. Bethe, Phys. Rev. 138(1965) B804

18) R. Rajaraman and H. A. Bethe, Rev. Mod. Phys. 39(1967) 745

19) B. D. Day, Phys. Rev. 187(1969) 1269

20) T. H. Schucan and H. A. Weidenmüller, Phys. Rev. C 3(1971) 1856

21) C. Mahaux, Nucl. Phys. A163(1971) 299

22) M. Gell-Mann and K. A. Brueckner, Phys. Rev. 106(1957) 364

23) K. A. Brueckner and K. Sawada, Phys. Rev. 106(1957) 1117

24) J. G. Zabolitzky, Nucl. Phys. A228(1974) 285

25) D. Ceperley, G. V. Chester and M. H. Kalos, Phys. Rev. B 16(1977) 3081

26) B. D. Day, F. Coester and A. Goodman, Phys. Rev. C 6(1972) 1992

27) B. D. Day, in preparation

28) V. R. Pandharipande, R. B. Wiringa and B. D. Day, Phys. Lett. 57B (1975) 205

29) K. R. Lassey and D. W. Sprung, Nucl. Phys. A177(1971) 125

30) V. R. Pandharipande and R. B. Wiringa, preprint

31) S. Fantoni and S. Rosati, Nuovo Cimento 25A(1975) 593

32) E. Krotscheck, J. Low Temp. Phys. 27(1977) 199

33) J. G. Zabolitzky, Phys. Rev. A 16(1977) 1258

34) K. E. Kürten, M. L. Ristig and J. W. Clark, Phys. Lett. 74B(1978) 153.

Figure Captions

1. Single-particle energy spectrum in nuclear matter.
2. Two-body relative wavefunctions in nuclear matter, as discussed in the text.
3. Two-hole-line diagram for the energy.
4. Some three-hole-line diagrams.
5. Three-body cluster diagrams.
6. Diagrammatic definition of the generalized ring vertex M.
7. The first two contributions to the energy from the generalized ring series. An additional diagram, obtained from (b) by omitting the interaction indicated by the arrow, is also included in the second-order term.
8. Calculated energy per particle plotted against Fermi momentum for v_2.
9. Calculated energy per particle plotted against Fermi momentum for v_6(Reid).

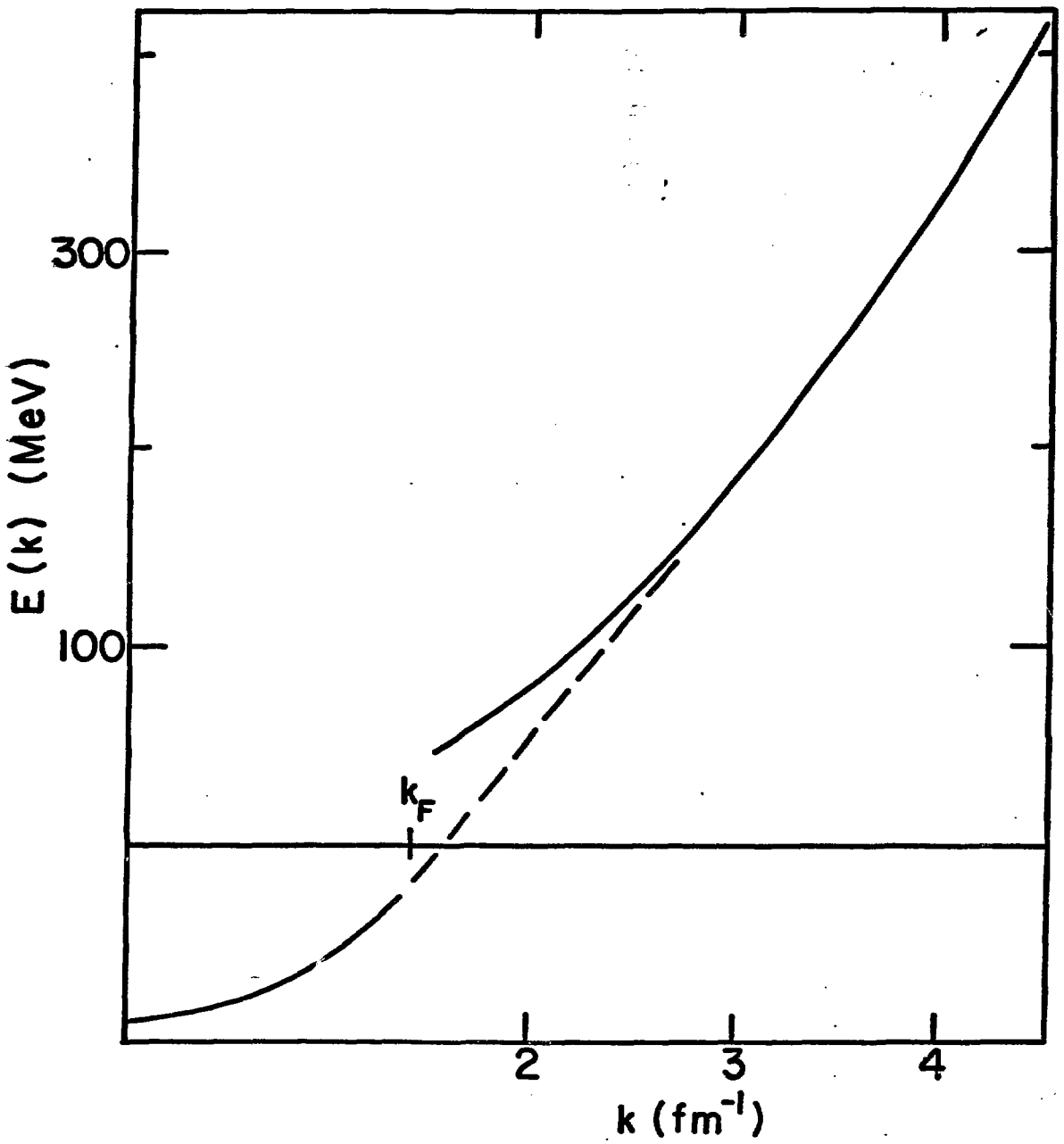

FIG. 1

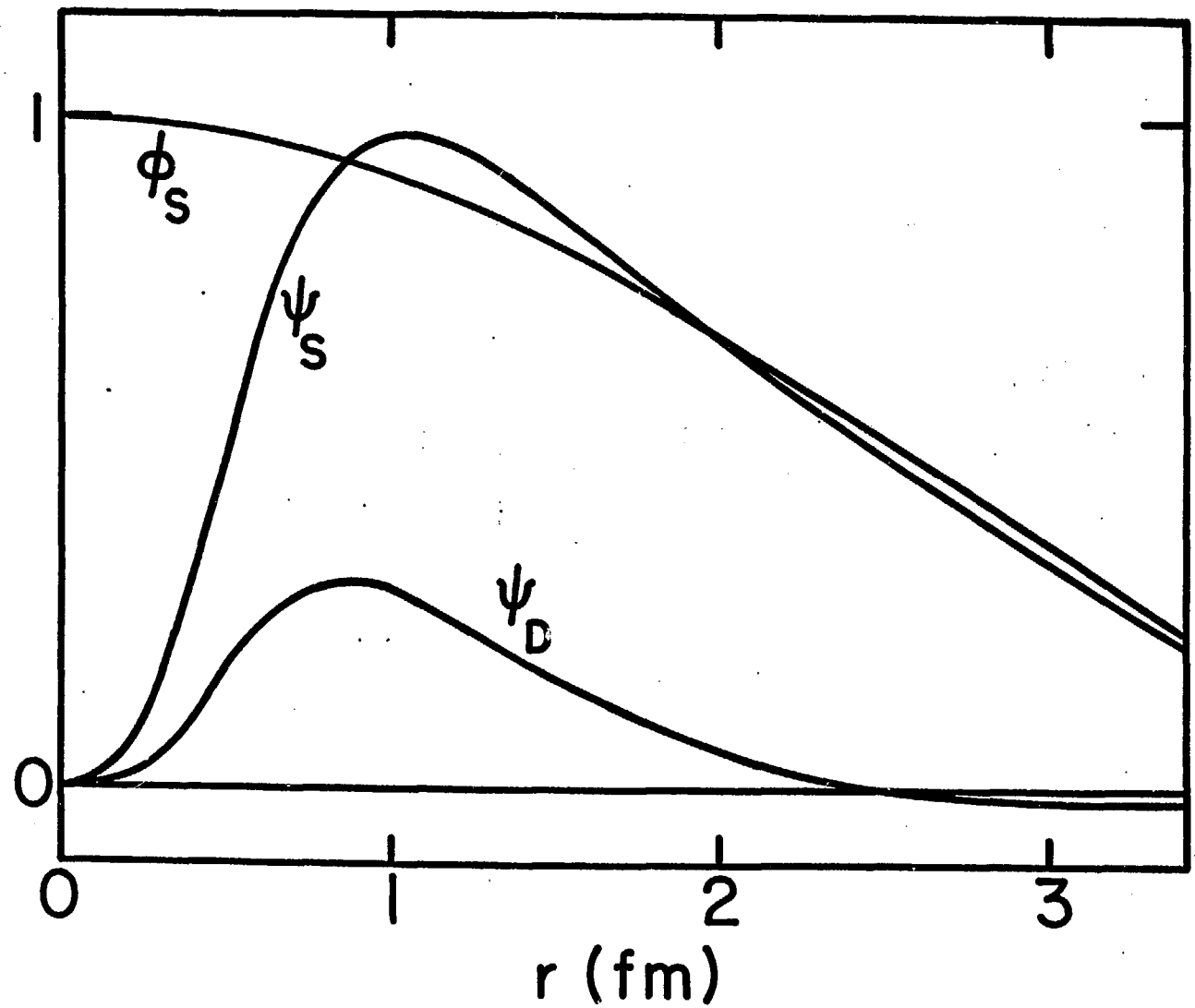

FIG. 2

FIG. 3

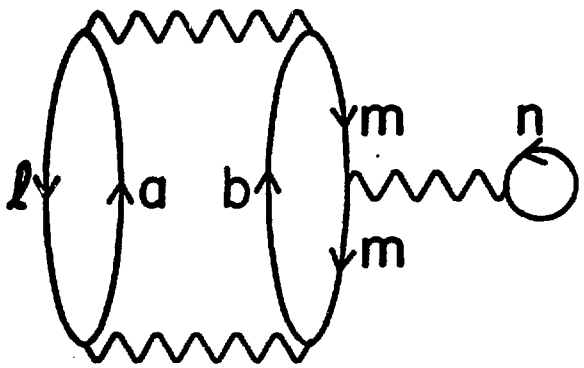

(a)

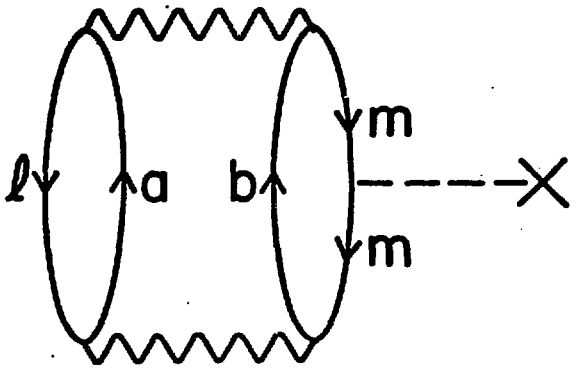

(b)

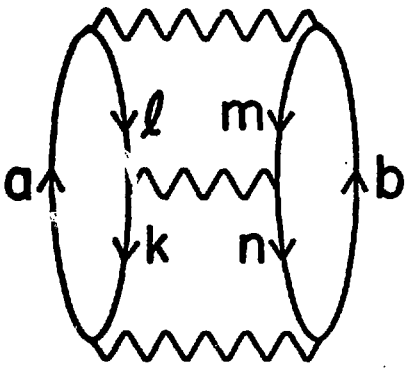

(c)

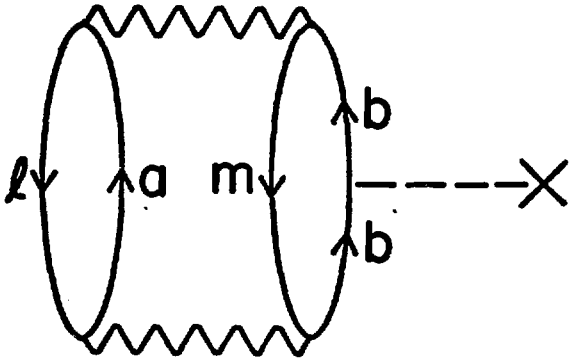

(d)

FIG. 4

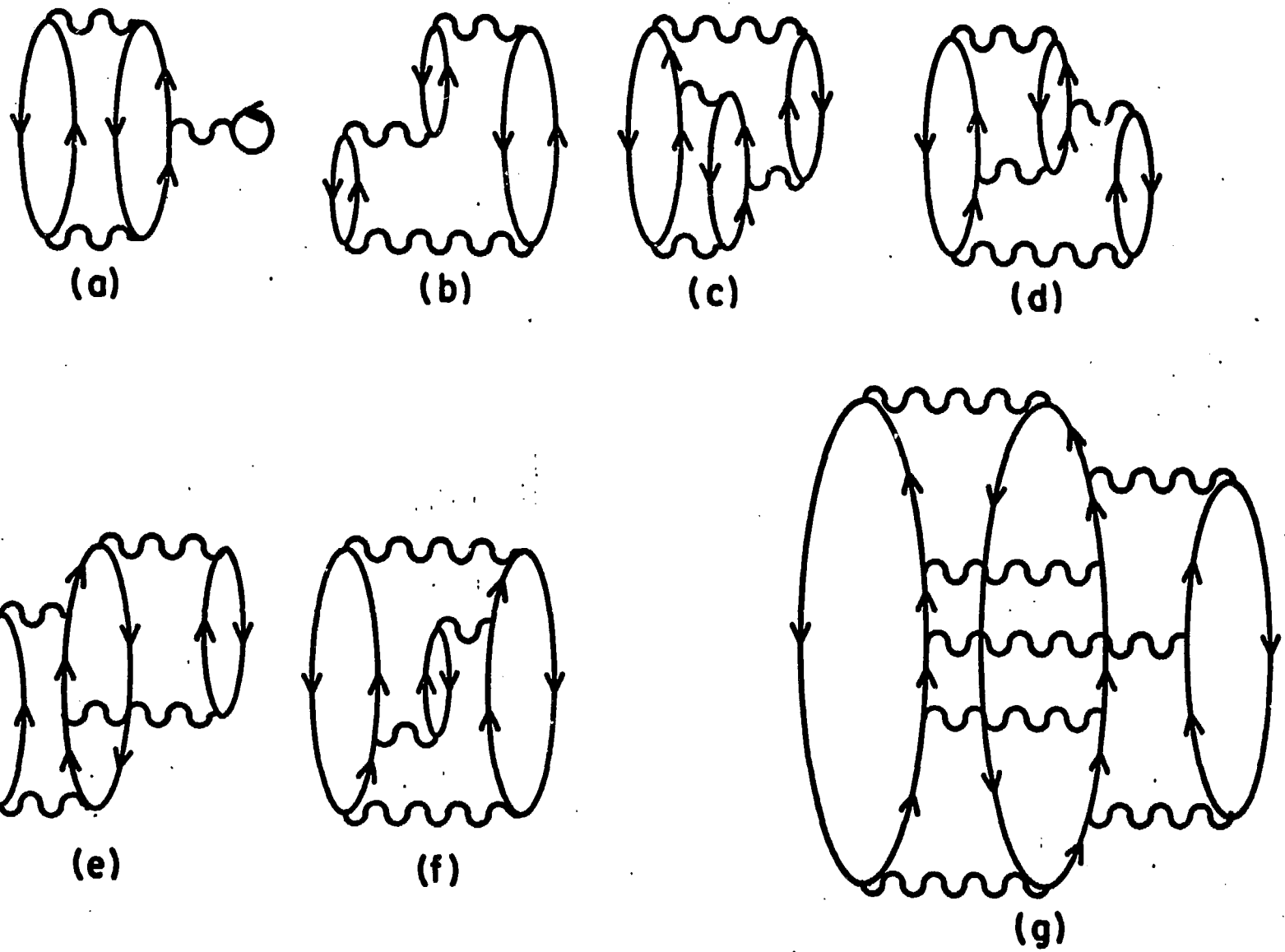

FIG. 5

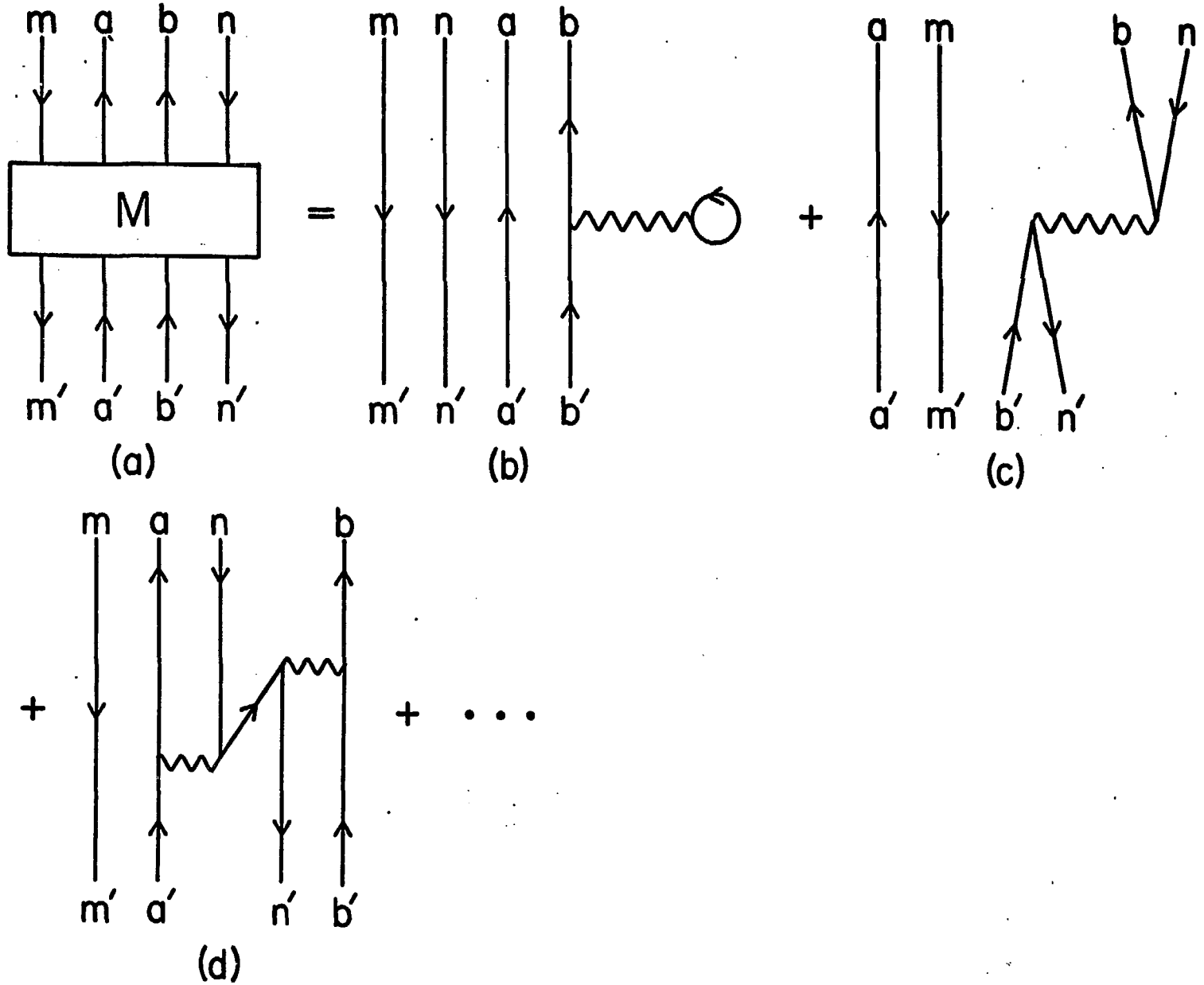

FIG. 6

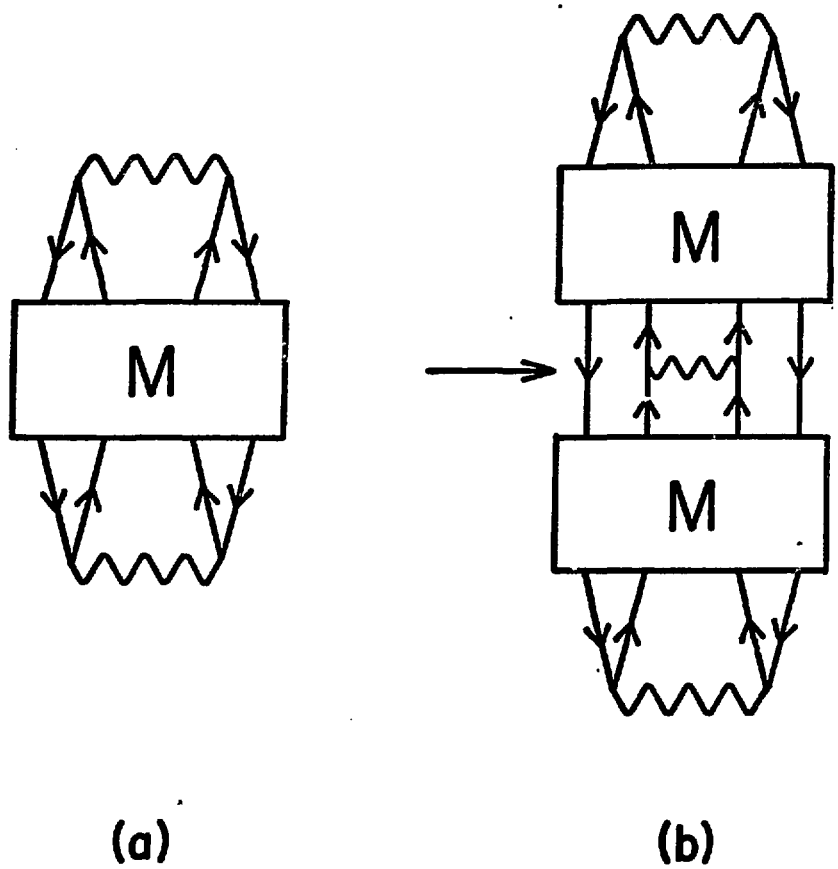

FIG. 7

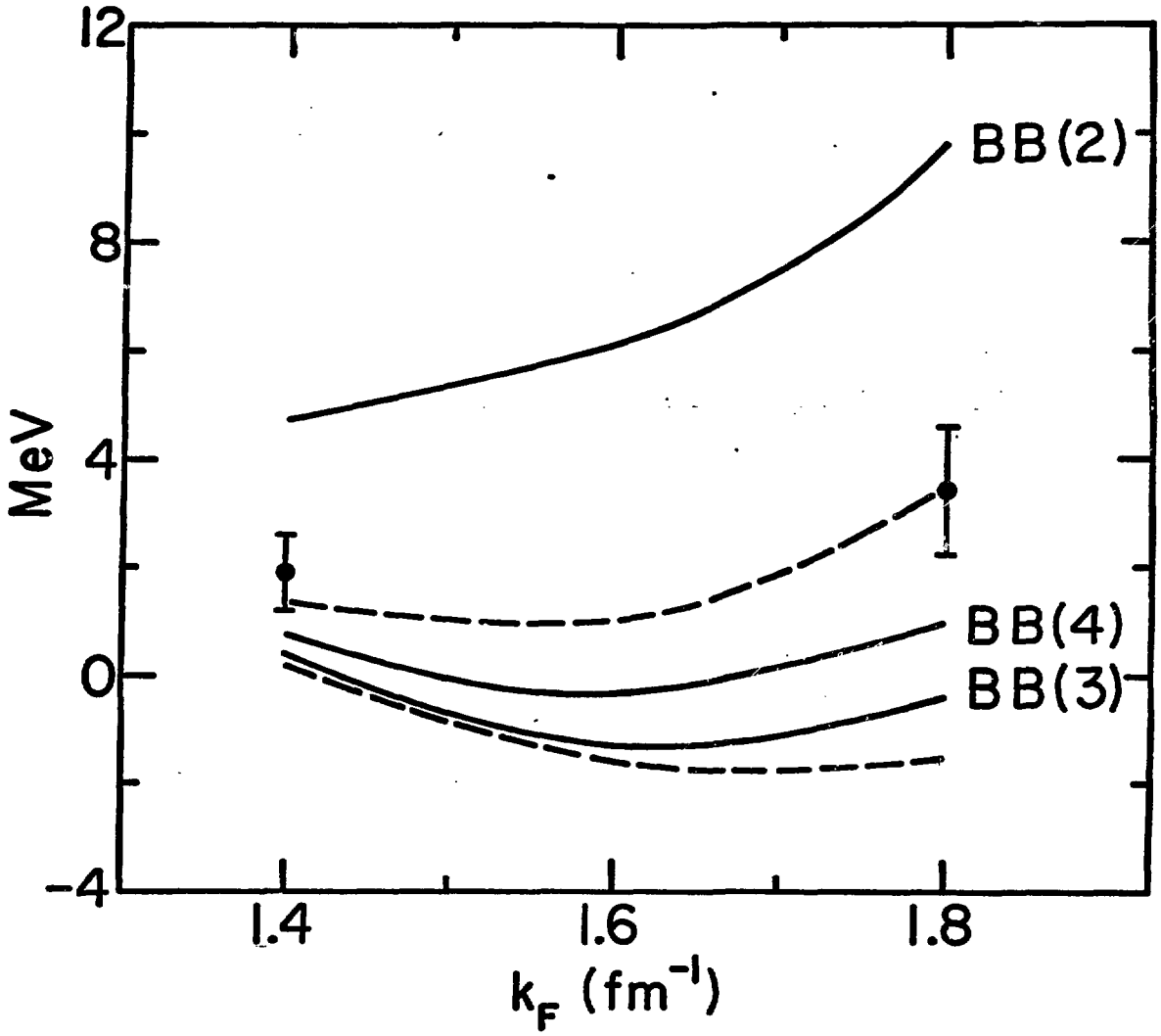

FIG. 8

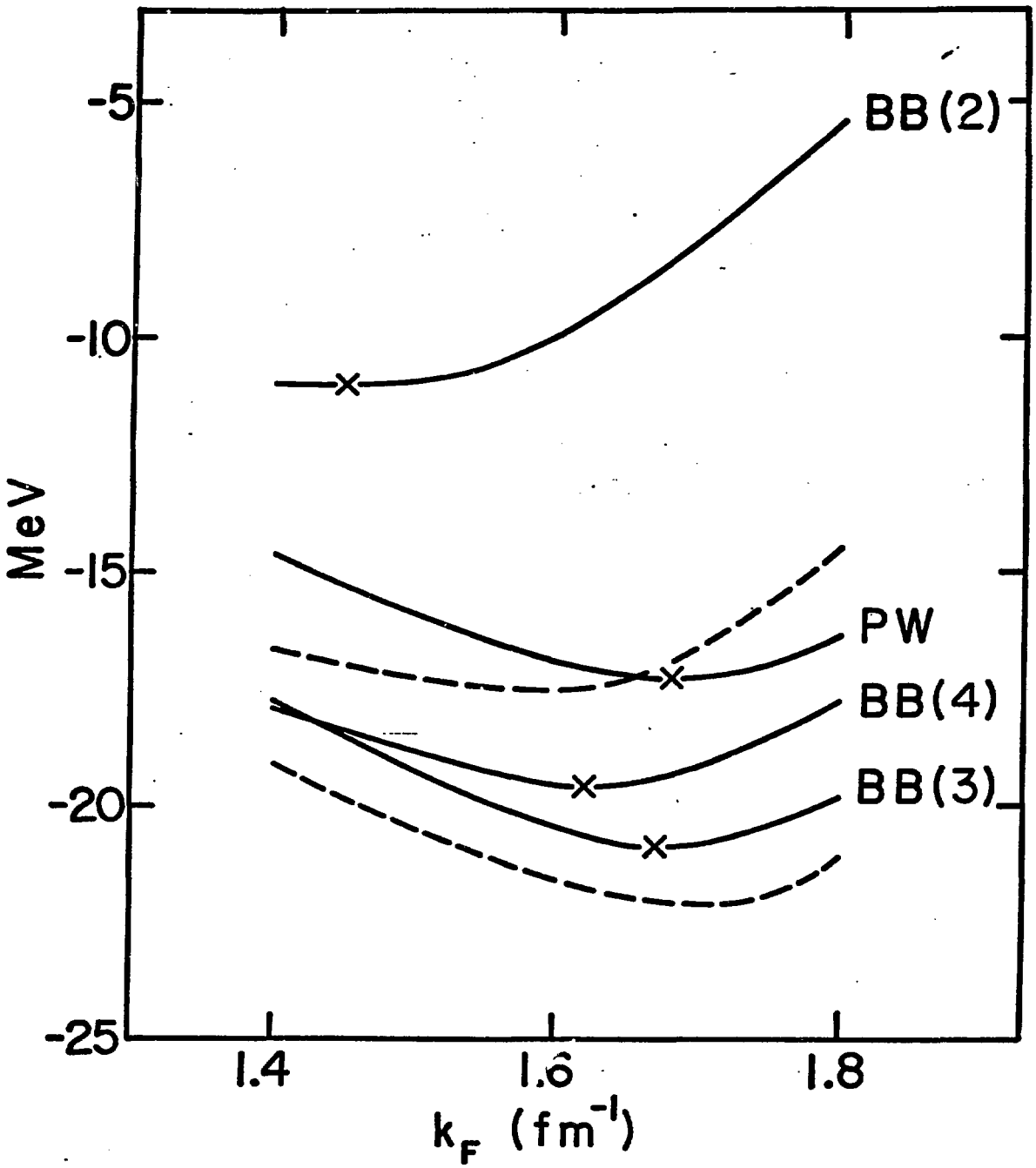

FIG. 9

BRUECKNER-BETHE CALCULATIONS OF NUCLEAR MATTER†

B. D. DAY

Argonne National Laboratory, Argonne, IL. 60439 USA*

Abstract: The ideas of the Brueckner-Bethe hole-line expansion are briefly outlined. Four practical tests of its validity are formulated. These tests are applied to recent numerical results for the central potential v_2 and the semirealistic potential v_6(Reid), which contains a tensor force but no spin-orbit force. The results are consistent with the validity of the hole-line expansion. The Brueckner-Bethe results are also consistent, within uncertainties of order 3 MeV, with variational results.

34 references

†Invited talk at the Conference on "Recent Progress in Many-Body Theories," October, 1978, at the International Center for Theoretical Physics, Trieste, Italy.

*Work performed under the auspices of the U. S. Dept. of Energy.